Research of chitosan coatings deposited by electrophoretic deposition method at various voltage and time parameters

Klaudia Malisz, Beata Świeczko-Żurek, Jean-Marc Olive, Gilles Pecastaings, Alina Sionkowska, Aleksandra Laska, Grzegorz Gajowiec

Research of chitosan coatings deposited by electrophoretic deposition method at various voltage and time parameters

Klaudia Malisz [1*], Beata Świeczko-Żurek [1], Jean-Marc Olive [2], Gilles Pecastaings [3] and Alina Sionkowska[4], Aleksandra Laska[5], Grzegorz Gajowiec[5]

[1] Department of Biomaterials, Faculty of Mechanical Engineering and Ship Technology, Technology, Gdansk University of Technology, Gabriela Narutowicza 11/12, 80-229 Gdansk, Poland; klaudia.malisz@pg.edu.pl, beata.swieczko-zurek@pg.edu.pl

[2] CNRS, Institute de Mecanique et d'Imgenierie, Universite de Bordeaux, 33405 Talence, France; jean-marc.olive@u-bordeaux.fr

[3] Centre de Recherche Paul Pascal, CNRS Universite de Bordeaux, UMR 5031, 33600 Pessac, France; gilles.pecastaings@crpp.cnrs.fr

[4] Faculty of Chemistry, Nicolaus Copernicus University in Torun, Gagarina 7, 87-100 Torun, Poland; alinas@umk.pl

[5] Department of Materials Science and Technology, Faculty of Mechanical Engineering and Ship Technology, Gdansk University of Technology Gabriela Narutowicza 11/12, 80-229 Gdansk, Poland; aleksandra.laska@pg.edu.pl, grzgajow@pg.edu.pl

*Correspondence: klaudia.malisz@pg.edu.pl

Abstract

The aim of this research is to estimate the electrophoretic deposition main parameters, such as voltage and time duration, that will provide optimal characteristics of the surface layer. Chitosan coatings were synthesized on biomedical Ti13Zr13Nb alloys at 20 V and 30 V and with deposit times of 2 min, 5 min, 10 min, and 15 min. Evaluation of the coating was performed by using Scanning Electron Microscope (SEM), Energy-Dispersive Spectroscopy (EDS), Laser-Induced Breakdown Spectroscopy (LIBS), Atomic Force Microscopy (AFM), drop shape analyzer and nanoscratch tester. Homogeneous and continuous coatings are obtained for 2 min and 5 min, regardless of the voltage. Defects in form of bubbles are observed only for 20 V during 10 min, 20 V during 15 min, and 30 V during 10 min. All of the coatings show hydrophilic behavior. The critical loads for delamination range are between 100 mN to 300 mN. It is concluded, that the optimal coating for orthopedic implants is obtained at 20 V, 5 minutes, because of homogeneity, a contact angle supporting osseointegration and the best adhesion. The optimal one for implant in contact with blood is obtained at 20 V, 2 minutes, because it is homogenous and shows the lowest hydrophilicity, which should limit the thrombogenicity of the coating.

Keywords: chitosan, titanium alloy, microscopic techniques, electrophoretic deposition, wettability, adhesion

1. Introduction

Titanium and its alloys are the most developed metallic biomaterials used for long-term orthopedic and dental implants [1,2]. The Ti13Zr13Nb alloy exhibits suitable mechanical properties, when compared to the most widely used technical titanium alloys, Ti6Al4V and Ti6Al7Nb. The absence of potentially harmful components like Al and V, which are thought to cause tissue disturbance and Alzheimer's disease, is one benefit of the Ti13Zr13Nb alloy [3,4]. Due to its non-toxicity and relatively low Young's modulus (about 80 GPa) [5], the Ti13Zr13Nb alloy appears to be the best choice in recent years [1].

Electrophoretic deposition (EPD) is one of many surface engineering techniques used to create bioactive and biocompatible coatings. A common EPD setup includes electrodes, a power supply, and a stable precursor suspension/solution. Once an electrical potential difference is established between the two electrodes, charged polymers or particles in the precursor solution will move under the influence of the electric field and deposit on the second electrode (oppositely charged electrode) to form a coating as a result. Mainly, electrophoretically deposited coatings are produced on non-degradable (stainless steel, titanium alloys, and cobalt-chromium alloys) or degradable (e.g. magnesium alloys) metals [6]. Electrophoretic deposition can be applied to any colloidal system with the suspended particles size smaller than 30 μm [7]. Commonly used EPD-deposited materials for therapeutic delivery include biopolymers, bioceramics, and carbon nanomaterials. In addition, composite coatings can be used to improve physicochemical and biological properties [6].

Using the EPD method scientists can create compact, porous coatings with excellent microstructural uniformity and controllable thickness [5]. Other benefits of EPD include, the requirement of simple equipment, room-temperature processing, and the possibility of forming coatings with complex shapes or patterns [5,8]. Particular attention should be paid to the solids content of the EPD precursor solution/suspension. EPD should be carried out at moderate voltages and concentrations to obtain uniform, dense and adhesive coatings without compromising the deposition rate. This is related to the fact that with too high a content of substances in the suspension, the homogeneity and adhesion strength of the coating decreases due to increased particle aggregation and reduced stability of the precursor solution. Another problem is the formation of bubbles when applying a strong DC electric field to aqueous suspensions. This phenomenon occurs during the hydrolysis of water, which has a detrimental effect on the quality (e.g. porosity and heterogeneity and low adhesive strength) of the deposit. There are several options to reduce this process during EPD, e.g. by adding ethanol or hydrogen peroxide into the precursor solution/suspension or by using pulsed direct current (DC) and alternating current (AC) power supply [6].

Chitosan is a natural, cationic polysaccharide and it can be obtained from the deacetylation reaction of chitin by chemical or enzymatic methods and is therefore al-so called deacetylated chitin [5,9]. Chitosan is a unique material that can be used in biomedical implants, drug delivery, scaffolds, biosensors, and other biomedical devices because of its exceptional biocompatibility, biodegradability, hemocompatibility, antibacterial activity, ability to protein adsorption, chemical stability, and ability to accelerate wound healing [5,10–13]. Additionally, chitosan has demonstrated many useful biological effects, such as lowering blood or liver cholesterol and triglyceride, immunostimulating effects, and antitumor and anti-inflammatory properties [14,15]. Chitosan has many medical applications, including the drag delivery to deeper tissues, which makes it useful for applications involving tissue regeneration. So, this biomaterial is a prospective substance for use in the biomedical field as well as in food manufacturing, biotechnology, pharmaceutical (e.g. drug delivery vehicles, carriers of immobilized enzymes and cells [16]), cosmetics industries, and environmental applications. Chitosan does have some disadvantages, the main one being its low solubility at pH 7.4, which

prevents it from being used in nasal or peroral medication delivery. The other one is fast swelling in the aqueous environment, which leads to immediate medicine release [5,13,17,18].

Mobika J. et al. [19] fabricated a biocompatible hydroxyapatite/silk fibroin/chitosan composite by using in-situ co-precipitation method. They established that chitosan content could accelerate the bioactivity of the composite. The maximum degradation rate was 30.28 ± 0.57% for the first week and 23.89 ± 0.58% for the second week, which confirms the composite's mineralization increase. Composite cytotoxicity was assessed using an osteoblast-like cell line, which confirmed that all composites are less toxic. The antibacterial properties of the material were also tested. Better antibacterial activity was obtained against Gram-negative, than against Gram-positive [19]. Sorkhi L. et al. [20] fabricated hydroxyapatite–chitosan–titania nanocomposite coatings on 316 L stainless steel by using EPD method. The results showed that the smoother coatings are produced when the titania to hydroxyapatite ratio is increased, a larger titania concentration causes cracking. Methanolic coatings offer greater corrosion resistance at low solids concentrations (hydroxyapatite and titania) due to their increased thickness, but lower corrosion resistance at higher solid concentrations due to cracks and rough surfaces [20].

However, Kumar S. et al. [11] synthesized chitosan xerogel, which could be used as a novel biodegradable material with improved antibacterial properties. Xerogels have excellent properties and can be used as biosensors, gene delivery, antimicrobials, and scaffolds for tissue regeneration. Disocyanate-modified chitosan (DIMC) was produced via a cross-linking reaction. They examined antibacterial properties against Escherichia coli and Staphylococcus pyogenes bacteria and claimed, that the DIMC showed a better degree of bacterial growth inhibition against E. coli than unaltered chitosan [11]. Varlık Ö. et al. [21] produced titanium diboride -chitosan composite coatings on titanium substrate using the EPD technique. They applied different voltage, time and solid concentration. Obtained coating was uniform, and crack-free. Different amount of chitosan is considered to have a significant effect on the adhesion to the substrate [21].

Kowalski P. et al. [22] compared the properties of chitosan coatings on a nitinol alloy (NiTi). EPD was performed at 10 V and settling time: 30, 60, 120, 300, 600 s. The results indicate that the use of a relatively low voltage and long deposition time, allow obtaining a homogeneous chitosan layer of a very similar thickness on the whole surface. An increase in voltage of up to 10 V combined with a longer deposition period causes the electrophoresis process to intensify. As a result, there is more evolved hydrogen present. It prevents chitosan particles from moving to the samples' surfaces, which has a significant impact on the topography of the chitosan surface. The layer becomes rough, and even cracking and peeling of chitosan fragments from the substrate occurs as a result [22].

Mohammadi F. et al. [23] developed the hybrid nanocomposite coating on NiTi to improve the blood compatibility, biocompatibility, and corrosion resistance of the metal. Firstly, they anodized the surface and then coated it with chitosan-heparin nanoparticles. The results showed a significant reduction in the nickel release, while promoting human umbilical vein endothelial cells attachment, spreading, and proliferation. However, by carefully controlling the release of heparin, the coating may considerably reduce blood coagulation [23]. Li P. et al. [24] also wanted to improve the properties of nitinol. They deposited chitosan/ag complex coating using EPD on biomedical NiTi alloy to enhance the antibacterial properties. The antibacterial activity of NiTi alloy (against the model bacterial E. coli) was remarkably improved by the complex coating [24].

In this work, chitosan coatings are prepared on biomedical Ti13Zr13Nb alloys by electrophoretic deposition using various parameters to compare its properties, such as wettability and adhesion of the coating to the substrate. The purpose of the comparison is to

determine the differences in coating properties depending on the deposition parameters, in order to obtain a coating with optimal properties for biomedical applications. No studies were found showing the effect of selected deposition parameters on the properties of chitosan coatings on the Ti13Zr13Nb alloy.

2. Material and methods

Chitosan coatings were deposited using the electrophoretic deposition (EPD) method on the Ti13Zr13Nb. The samples had a diameter of 20 mm and a height of 3 mm. The surface was prepared by using abrasive paper SiC up to grit # 2500. The samples were washed with distilled water and dried with compressed air.

The electrolyte used for the deposition includes 0.104 g of high molecular weight chitosan, 100 ml of distilled water, and 1 ml of 99.5% acetic acid. The electrolyte were homogenized using a magnetic stirrer (at 600 rpm) for 5 hours at room temperature. The suspension was prepared immediately before deposition. The titanium alloy substrate was used as a cathode and platinum as a counter electrode. The electrodes were parallel to each other at a distance of 10 mm and connected to a power source. A DC power source (MCP/SPN110-01C, Shanghai MCP Corp., Shanghai, China) was applied. The EPD was performed at 20 V and 30 V for 2, 5, 10 and 15 min (details can be found in Table 1). The deposition was carried out at room temperature. Finally, chitosan coatings were air-dried at room temperature for 48 h.

The morphology and quality of the coatings were assessed by scanning electron microscopy (JEOL JSM- 7800F, JEOL Ltd., Tokyo, Japan). Observation was made using a secondary electron detector at acceleration voltage of 1 kV and 5 kV. The chemical composition of the resulting coatings was analyzed by an energy dispersive X-ray spectrometer (EDS Edax Inc., Mahwah, NJ,U.S.A.) and Laser Induced Breakdown Spectroscopy (Keyence, VHX-7000, Osaka, Japan). EDS analysis was performed on the sample surface area at 500x magnification. The analyzes carried out were intended to confirm the presence of carbon and oxygen, and thus the presence of a coating on the sample surface. AFM (Dimension Icon, Bruker, Germany) in tapping mode with RTESPA-300 probes (spring constant 40N/m, resonance frequency 350kHz) was used to assess the thickness of coatings. The coating on half of the sample was mechanically removed, and then its thickness was examined in several places (on the border between the coating and the substrate). From topographic images, Nanoscope Analysis software (Bruker) was used to obtain line profiles of step height analysis. The roughness of the deposit was also examined using AFM. The measurements were carried out on a small area (2μm x 2μm).

The wettability of the coatings (n = 5 for samples) was evaluated by the falling drop method using water (1.8 μl) at room temperature (Optical Tensiometr Attension, Theta Lite, Biolin Scientific, Sweden). The computer program analyzed the contact angle (CA) for 10 s.

Nanoscratch tests were conducted with a nanoindenter (NanoTest Vantage, Micro Materials, Wrexham, UK). The scratch tests were repeated 10 times while increasing the load from 0mN to 400mN at the load rate of 2.0mN/s at a distance of 500μm. The location of delamination was determined, based on SEM images and changes in frictional force during the test.

Table 1. Sample designation and deposition conditions.

Sample	Voltage [V]	Time [min]	Sample	Voltage [V]	Time [min]
CH20/2	20	2	CH30/2	30	2
CH20/5	20	5	CH30/5	30	5
CH20/10	20	10	CH30/10	30	10
CH20/15	20	15	CH30/15	30	15

3. Results and Discussion

3.1. Microstructure and Morphology of Chitosan

SEM images of surface are presented in the pictures Fig. 1 and Fig. 2. In the case of coatings deposited for 2 minutes, and CH30/15 microstructure was continuous and homogeneous. However, microscopic observations revealed traces in the coatings of these precipitated bubbles. Single bubbles at the edges are visible on the CH20/5 coating. Moreover, the coatings CH20/10, CH20/15, and CH30/10 have a fully bubbly microstructure. Additionally, numerous undissolved fragments of chitosan were visible on the surface of the samples, filtering may be a potential solution to this problem.

The phenomenon of the formation of cavities on the coating is well-known among scientists. On the cathode, water electrolysis occurs, which results in the release of OH^- and the formation of H_2 bubbles. As a result, the localized pH value near the cathode is increased which deprotonates the chitosan for film formation. It should be highlighted that a typical chitosan film made from EPD exhibits poor homogeneity and numerous surface crevices created by the trapped H_2 bubbles. Therefore, the resulting chitosan film often lacks acceptable mechanical strength to be free-standing [25]. One method of reducing the formation of hydrogen bubbles that affect the homogeneity of the coatings is to reduce the water content in the EPD suspension [26]. Additionally, the increasing content of chitosan in the EPD suspension could form bubbles that adhere to the deposited coating, increasing its porosity [26,27]. Furthermore, the smoothest coatings were obtained at the lowest deposition time and voltage value [26,28].

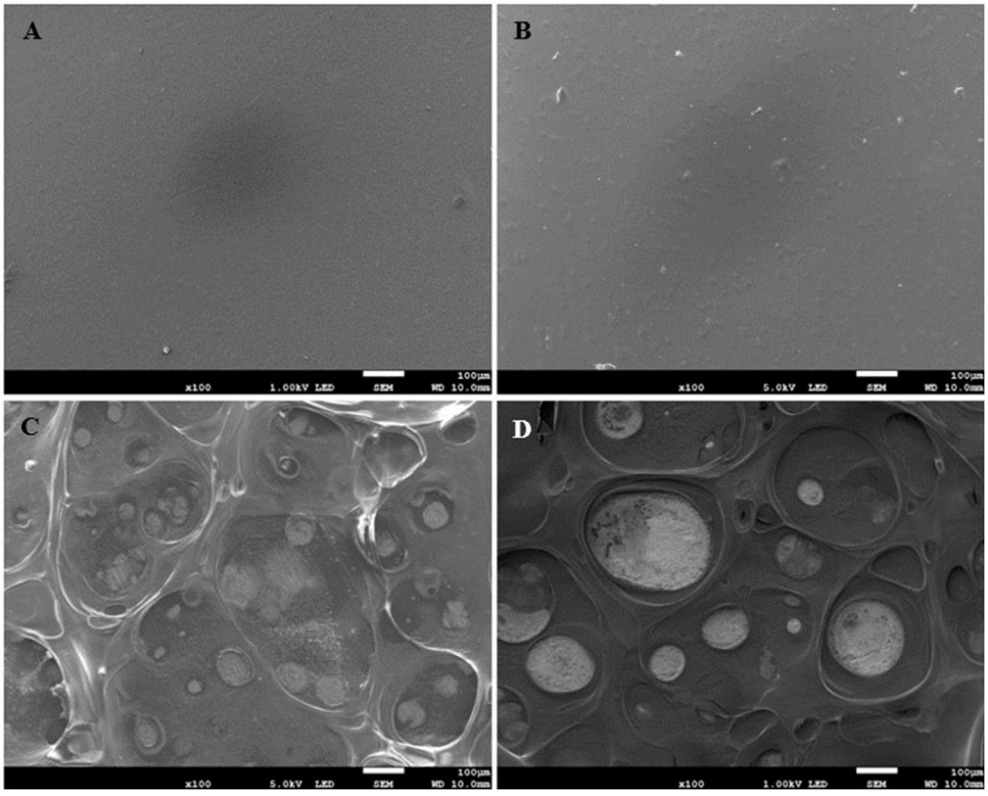

Fig. 1. Chitosan coatings: A) CH20/2; B) CH20/5; C) CH20/10; D)CH20/15.

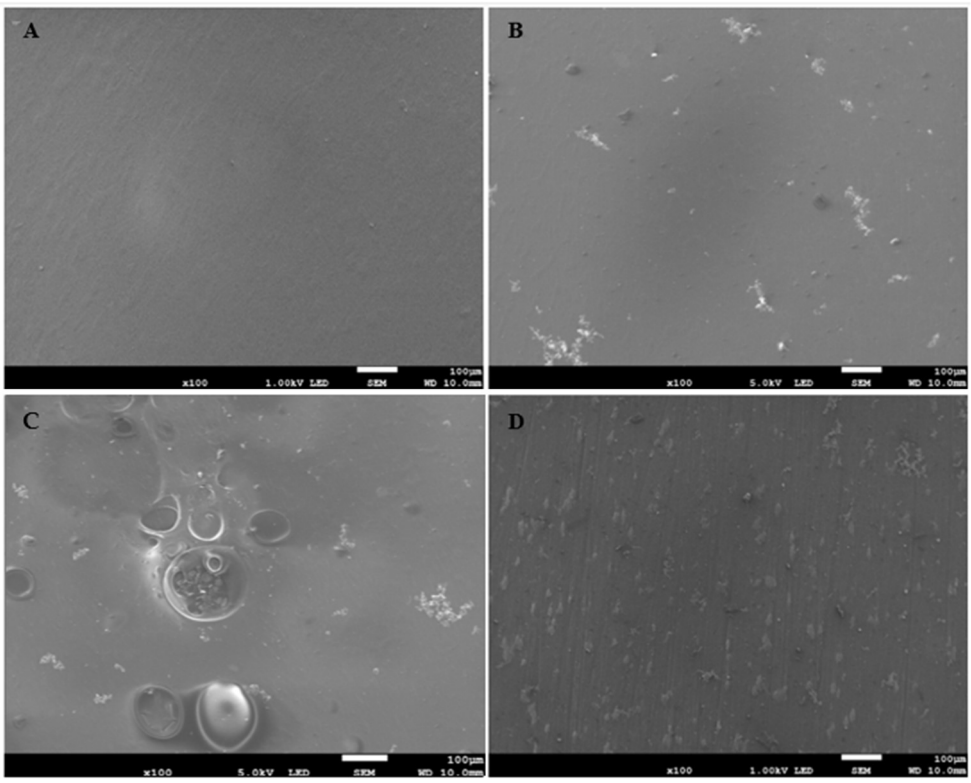

Fig. 2. Chitosan coatings: A) CH30/2; B) CH30/5; C) CH30/10; D) CH30/15.

The qualitative EDS (Fig. 3) and LIBS analysis of the sample's surface was performed. EDS revealed the presence of typical elements relating to the substrate (Ti) and the elements of which the composite coating was composed (C, O, N). The detection of H content is not possible for that technique.

The results of the LIBS analysis (Fig. 4) showed a predominance of the organic component (chitosan: $(C_6H_{11}NO_4)n$) as well as the presence of the substrate (Ti), titanium alloy components (Nb, Zr) did not always appear in the analysis. The detection sensitivity for N is poor by conventional atomic LIBS [29], therefore the examination did not show nitrogen content. Measurements were taken in 10 different locations and the presented measurements do not show significant differences in composition.

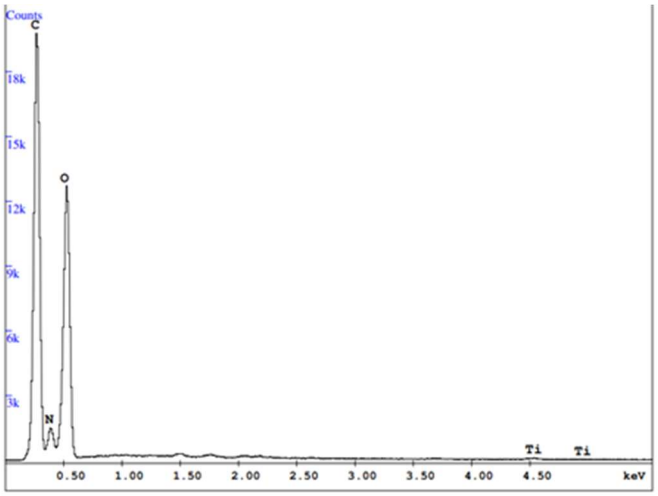

Fig. 3. EDS spectrum for chitosan coating.

A)

Multi-point analysis [wt%]

No.	Presumed material	Ti	O	C	Zr	Nb	H	
1	Titanium compound	34.2%	32.4%	12.1%	9.3%	7.1%	4.9%	
2	Titanium compound	36.1%	27.8%	12.6%	11.9%	7.2%	4.4%	
3	Titanium compound	33.8%	36,0%	10.9%	9,0%	5.9%	4.4%	
4	Titanium compound	31.5%	36.3%	9.9%	10.8%	6.7%	4.8%	
5	Titanium compound	40.2%	27.2%	10.1%	11.8%	7.2%	3.5%	
6	Titanium compound	34.9%	31.1%	12.4%	10.6%	6.7%	4.3%	
7	Titanium compound	40,0%	25.4%	10.8%	13.2%	7,0%	3.6%	
8	Titanium compound	37.6%	27.7%	11.6%	11.4%	7.7%	4,0%	
9	Titanium compound	34.6%	28.3%	11.5%	12.5%	8.7%	4.4%	

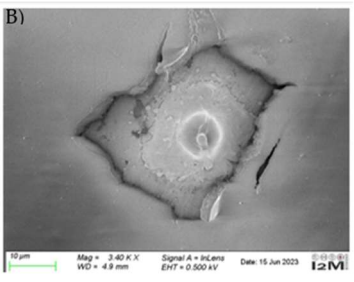

Fig. 4. LIBS analysis of coating, table with elements compound (A), SEM image after LIBS (B).

Surface roughness was assessed using AFM. Results are presented in Table 2. and Figure 5. The coatings have the same chemical composition and differ only in thickness, which suggests that they should have the same surface roughness. Possible differences in coating roughness may result from the microstructure of the base material, bubble formation, and undissolved polymer fragments foreign to the surface. However, the measurements were carried out on a small area (2µm x 2µm) to avoid the influence of defects on the roughness of the microstructure. Due to the expected similar results, the tests were carried out on two samples with extreme deposition parameters and on the sample with the thickest coating. Based on Rq (root mean square roughness), no significant difference in surface roughness was found.

Table 2. Results of the roughness.

	CH20/2	**CH20/5**	**CH30/15**
Rq [nm]	2.5	2.6	2.7

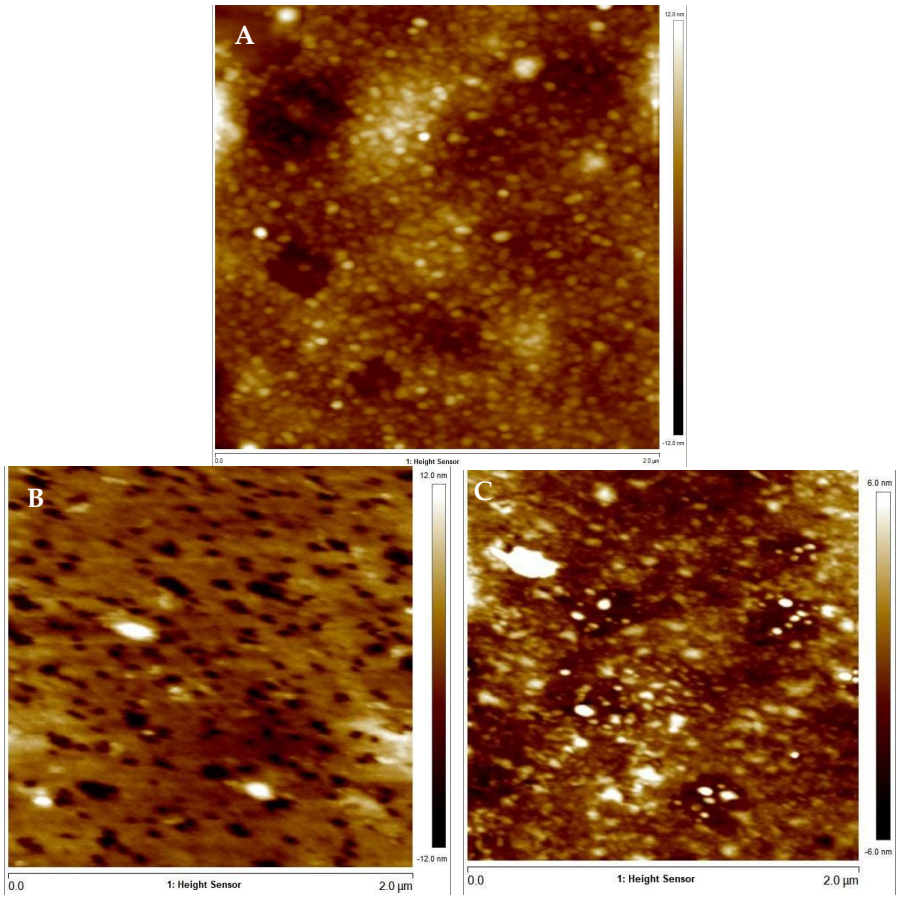

Fig. 5. AFM images of surface; A) CH20/2, B) CH20/5, C) CH30/15.

The thickness of coatings is presented in Table 3 and the AFM image of CH20/5 is in Fig. 6. The known kinetics of the reaction and the relationship between the deposition time and the weight of the coating on the surface of the sample indicates that with increasing time, more chitosan weight per area is obtained [30]. The research confirmed, that the thickness of coatings will increase with time. There was also an increase in the thickness of the coatings with a deposition time of 5 minutes and a voltage change from 20 to 30V. The fact, that the coated layer thickness grew with the raising of the applied voltage, is known in the literature [31]. Regardless of the voltage, coatings deposited at 2 and 5 minutes have a non-uniform thickness over the entire surface.

Moreover, with the raising of the deposition time, the rate of coating may reach zero [31]. In addition, longer deposition time leads to intensification of the process of electrophoresis and that increases the amount of hydrogen. It has a significant influence on coating because it blocks the flow of chitosan particles to the surface of the samples. This phenomenon indicates, that the chitosan surface becomes rough, and even cracking and peeling of fragments of the chitosan from the substrate occurs [22]. Probably for this reason why very thin coatings were obtained at 15 min. Besides, the continuous formation of cavities might reduce the amount of chitosan on the surface, but this coating is the most homogenous in thickness.

Table 3. Thickness value of chitosan coatings obtained using AFM.

Sample	Average Thickness [µm]
CH20/2	2.5 ± 1.0
CH20/5	2.8 ± 0.9
CH30/2	1.5 + 0.4
CH30/5	3.9 ± 1.2
CH30/10	4.5 ± 0.4
CH30/15	1.8 ± 0.1

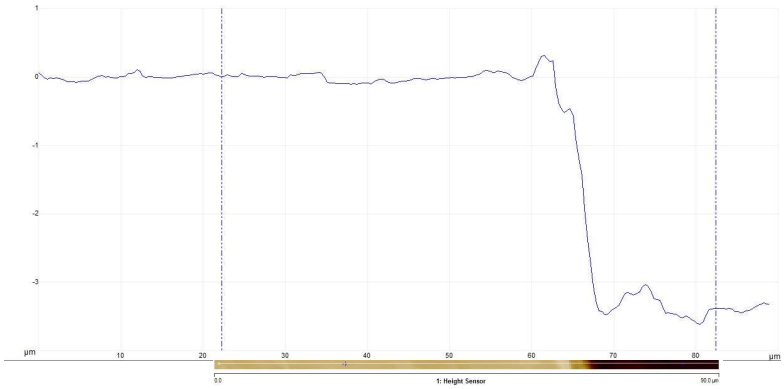

Fig. 6. AFM image and profile to assess the thickness of the coating CH20/5.

3.2. Wettability test

Wettability tests were carried out using the Attension Thete Lite goniometer. Table 4 presents the average value of CA after 10 ± 0.07 s. All coatings, except CH20/2, are hydrophilic. The lowest average contact angle was obtained in the case of CH30/10 and the highest was found in the sample CH20/2.

A crucial aspect influencing protein adsorption, bacterial and cell adhesion, platelet adhesion, and blood coagulation is the wettability of biomaterials. According to several research, the contact angle of the coatings should be between 40° and 60° for the best adhesion of cells. However, this range could vary depending on the cell type. This range is described for bone

cells as 35°- 85°, with 55° being the ideal value [1,26,32]. In the case of vascular implants, the hydrophobic surface frequently inhibits the adsorption of blood cells [33]. All samples that were tested therefore came very near to meeting these requirements. For applications on implants having contact with blood, the best value of the contact angle has CH20/2.

Table 4. The value of the average contact angle.

Sample	Average CA [º]	Sample	Average CA [º]
CH20/2	92 ± 3	CH30/2	72 ±10
CH20/5	78 ± 6	CH30/5	75 ± 3
CH20/10	81 ± 3	CH30/10	71 ± 2
CH20/15	82 ± 4	CH30/15	72 ± 5

3.3. Nanoscratch-test

Adhesion of the coatings to the metallic substrate was assessed by scratch test and SEM images. Results are presented in Table 5 and Fig. 7. Uncertainties (S) were estimated from standard deviation (S_x) and experimenter uncertainty (S_{ex}) (assumed mistake: 12mN, S_{ex}=6.9) using (1).

$$S = \sqrt{\frac{1}{3}{S_{ex}}^2 + {S_x}^2} \quad (1)$$

It is challenging to calculate coating cohesion forces for polymeric materials. Coating adhesion is able to be assessed in the scratch test experiment after the coating completely separated from the titanium substrate [26]. The best adhesion was characteristic for the CH20/5 coating, and the lowest force needed to delamination the coating was observed in the case of CH20/2. The increase in the deposition time is associated with the change in the thickness of the coating. Based on tests of coatings deposited at 30V, it can be concluded that increasing the deposition time to 15 min negatively affects the adhesion of the obtained coating. All nanoscratch test results showed damage of the coating at the coating-metal interface, indicating adhesive failure.

Table 5. Nanoscratch test results.

Sample	Critical load (mN)
CH20/2	103 ± 20
CH20/5	316 ± 34
CH20/10	Not performed because of bubble microstructure
CH20/15	Not performed because of bubble microstructure
CH30/2	247 ± 27
CH30/5	164 ± 20
CH30/10	223 ± 37
CH30/15	133 ± 25

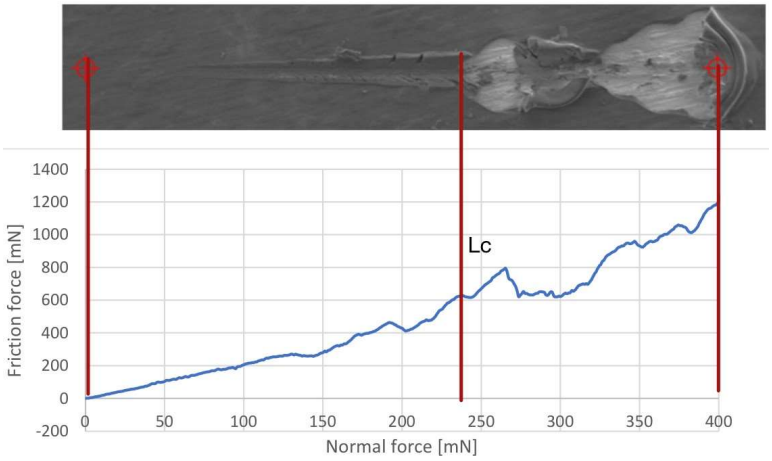

Fig. 7. Nanoscratch-test curves for chitosan coating (CH30/10) with marked delamination force (Lc).

4. Conclusions

Chitosan coatings were successfully deposited on Ti13Zr13Nb alloy by EPD process. The deposition was carried out for 2 min, 5 min, 10 min, and 15 min applying voltages of 20 and 30 V. Microscopic examinations, wettability tests, and adhesion assessments were carried out. The structure was continuous and homogeneous or there were visible bubbles formed as a result of water hydrolysis. Almost all samples showed hydrophilic properties. They were characterized by good adhesion. Based on the conducted research, it can be concluded that increasing the deposition time to 10 min and 15 min negatively affects the properties of the coatings.

The optimal coating for orthopedic implants would be CH20/5 because it showed continuity, homogeneity, a contact angle supporting osseointegration (78 ± 6°), and the best adhesion (delamination of the coating at a force of 316 ± 34 mN, and thickness 2.8 ± 0.9 µm. For applications on implants having contact with blood, the best property has CH20/2, because it is homogenous and shows the lowest hydrophilicity (contact angle is 92 ± 3°), which should limit the thrombogenicity of the coating. Moreover, the adherence of the coating to the metal substrate is sufficient.

Formatting of funding sources

This research did not receive any specific grant from funding agencies in the public, commercial, or not-for-profit sectors.

Author contributions

Conceptualization: Klaudia Malisz, Beata Świeczko-Żurek; Methodology: Klaudia Malisz, Beata Świeczko-Żurek, Gilles Pecastaings, Grzegorz Gajowiec, Aleksandra Laska; Formal analysis and investigation: Klaudia Malisz, Jean-Marc Olive, Gilles Pecastaings; Writing - original draft preparation: Klaudia Malisz; Writing - review and editing: Beata Świeczko-Żurek, Jean-Marc Olive, Alina Sionkowska; Supervision: Beata Świeczko-Żurek, Jean-Marc Olive, Alina Sionkowska.

References

[1] M. Bartmanski,, B. Cieslik, J. Glodowska, P. Kalka, L. Pawlowski, M. Pieper, A. Zielinski, Electrophoretic Deposition (EPD) of Nanohydroxyapatite - Nanosilver Coatings on Ti13Zr13Nb Alloy, Ceram. Int. 43 (2017) 11820–11829. https://doi.org/10.1016/j.ceramint.2017.06.026.

[2] S. Prasad, M. Ehrensberger, M.P. Gibson, H. Kim, E.A. Monaco, Biomaterial Properties of Titanium in Dentistry, J. Oral Biosci. 57 (2015) 192–199. https://doi.org/10.1016/j.job.2015.08.001.

[3] M. Bartmanski, A. Zielinski, B. Majkowska-Marzec, G. Strugala, Effects of Solution Composition and Electrophoretic Deposition Voltage on Various Properties of Nanohydroxyapatite Coatings on the Ti13Zr13Nb Alloy, Ceram. Int. 44 (2018) 19236–19246. https://doi.org/10.1016/j.ceramint.2018.07.148.

[4] K. Malisz, B. Świeczko-Żurek, Biological and Mechanical Research of Titanium Implants Covered with Bactericidal Coating, Eng. Biomater. 165 (2022) 17–22. https://doi.org/10.34821/eng.biomat.165.2022.17-22.

[5] D. Jugowiec, A. Łukaszczyk, Ł. Cieniek, M. Kot, K. Reczyńska, K. Cholewa-Kowalska, E. Pamuła, T. Moskalewicz, Electrophoretic Deposition and Characterization of Composite Chitosan-Based Coatings Incorporating Bioglass and Sol-Gel Glass Particles on the Ti-13Nb-13Zr Alloy, Surf. Coatings Technol. 319 (2017) 33–46. https://doi.org/10.1016/j.surfcoat.2017.03.067.

[6] X. Cheng, Y. Liu, O. Liu, Y. Lu, Z. Liao, Z. Hadzhieva, L. Chen, S.G.C. Leeuwenburgh, A.R. Boccaccini, F. Yang, Electrophoretic Deposition of Coatings for Local Delivery of Therapeutic Agents, Prog. Mater. Sci. 136 (2023) 101111. https://doi.org/10.1016/j.pmatsci.2023.101111.

[7] Y. Ma, J. Han, M. Wang, X. Chen, S. Jia, Electrophoretic Deposition of Graphene-Based Materials: A Review of Materials and Their Applications, J. Mater 4. (2018) 108–120. https://doi.org/10.1016/j.jmat.2018.02.004.

[8] C. Wang, J. Ma, W. Cheng, R. Zhang, Thick Hydroxyapatite Coatings by Electrophoretic Deposition, Mater. Lett. 57 (2002) 99–105. https://doi.org/1016/S0167-577X(02)00706-1.

[9] W. Tang, J. Wang, H. Hou, Y. Li, J. Wang, J. Fu, L. Lu, D. Gao, Z. Liu, F. Zhao, et al., Review: Application of Chitosan and Its Derivatives in Medical Materials, Int. J. Biol. Macromol. 240 (2023) 124398. https://doi.org/10.1016/j.ijbiomac.2023.124398.

[10] D. Zhitomirsky, J.A. Roether, A.R. Boccaccini, I. Zhitomirsky, Electrophoretic Deposition of Bioactive Glass/Polymer Composite Coatings with and without HA Nanoparticle Inclusions for Biomedical Applications, J. Mater. Process. Technol. 209 (2009) 1853–1860. https://doi.org/10.1016/j.jmatprotec.2008.04.034.

[11] S. Kumar, V. Deepak, M. Kumari, P.K. Dutta, Antibacterial Activity of Diisocyanate-Modified Chitosan for Biomedical Applications, Int. J. Biol. Macromol. 84 (2016) 349–353. https://doi.org/10.1016/j.ijbiomac.2015.12.027.

[12] S. Kumar, J. Koh, Physiochemical, Optical and Biological Activity of Chitosan-Chromone Derivative for Biomedical Applications, Int. J. Mol. Sci. 13 (2012) 6102–6116.

[13] T. Singh, S. Singh, G. Singh, Fabrication and Characterization of Chitosan – Hydroxyapatite – Zirconium Dioxide Composites for Biomedical Applications, Mater. Today Proc. 26 (2020) 1878–1883. https://doi.org/10.1016/j.matpr.2020.02.411.

[14] S. (Gabriel) Kou, L. Peters, M. Mucalo, Chitosan: A Review of Molecular Structure, Bioactivities and Interactions with the Human Body and Micro-Organisms, Carbohydr. Polym. 282 (2022) 119132. https://doi.org/10.1016/j.carbpol.2022.119132.

[15] S.-I. Ahn, S. Cho, N.-J. Choi, Effectiveness of Chitosan as a Dietary Supplement in Lowering Cholesterol in Murine Models: A Meta-Analysis, Mar. Drugs. 19 (2021) 26. https://doi.org/10.3390/md19010026.

[16] S. Kumar, J. Dutta, P.K. Dutta, Preparation and Characterization of N-Heterocyclic Chitosan Derivative Based Gels for Biomedical Applications, Int. J. Biol. Macromol. 45 (2009) 330–337. https://doi.org/10.1016/j.ijbiomac.2009.08.002.

[17] P.P. Sharma, S. Bhardwaj, A. Sethi, V.K. Goel, M. Grishina, Poonam, B. Rathi, Chitosan Based Architectures as Biomedical Carriers, Carbohydr. Res. 522 (2022) 108703. https://doi.org/ 10.1016/j.carres.2022.108703.

[18] R. Jayakumar, M. Prabaharan, R.L. Reis, J.F. Mano, Graft Copolymerized Chitosan—Present Status and Applications, Carbohydr. Polym. 62 (2005) 142–158. https://doi.org/10.1016/j.carbpol.2005.07.017.

[19] J. Mobika, M. Rajkumar, V. Nithya Priya, S.P. Linto Sibi, Effect of Chitosan Reinforcement on Properties of Hydroxyapatite/Silk Fibroin Composite for Biomedical Application, Phys. E Low-dimensional Syst. Nanostructures. 131 (2021) 114734. https://doi.org/10.1016/j.physe.2021.114734.

[20] L. Sorkhi, M. Farrokhi-Rad, T. Shahrabi, Electrophoretic Deposition of Hydroxyapatite–Chitosan–Titania on Stainless Steel 316 L, Surfaces. 2 (2019) 458-467. https://doi.org/10.3390/surfaces2030034.

[21] Ö. Varlık, Y. Göncü, N. AY, Electrophoretic deposition of composite titanium diboride-chitosan coating, Mater. Chem. Phys. 282 (2022) 125927. https://doi.org/10.1016/j.matchemphys.2022.125927

[22] P. Kowalski, B. Łosiewicz, T. Goryczka, Deposition of Chitosan Layers on NiTi Shape Memory Alloy, Arch. Metall. Mater. 1 (2015) 171–176. https://doi.org/10.1515/amm-2015-0027.

[23] F. Mohammadi, N. Golafshan, M. Kharaziha, A. Ashrafi, Chitosan-Heparin Nanoparticle Coating on Anodized NiTi for Improvement of Blood Compatibility and Biocompatibility, Int. J. Biol. Macromol. 127 (2019) 159–168. https://doi.org/10.1016/j.ijbiomac.2019.01.026.

[24] P. Li, X. Zhang, R. Xu, W. Wang, X. Liu, K.W.K. Yeung, P.K. Chu, Electrochemically Deposited Chitosan/Ag Complex Coatings on Biomedical NiTi Alloy for Antibacterial Application, Surf. Coatings Technol. 232 (2013) 370–375. https://doi.org/10.1016/j.surfcoat.2013.05.037.
[25] B.-H. Huang, L.-J. Chen, Y.-J. Chiou, G. Whang, Y. Luo, Y. Yan, K.-H. Wei, X. He, B. Dunn, P.-W. Wu, Bubble-Channeling Electrophoresis of Honeycomb-Like Chitosan Composites, Adv. Sci. 9 (2022) 2203948 https://doi.org/10.1002/advs.202203948.
[26] Ł. Pawłowski, M. Bartmański, A. Mielewczyk-Gryń, B.M. Cieślik, G. Gajowiec, A. Zieliński, Electrophoretically Deposited Chitosan/Eudragit E 100/AgNPs Composite Coatings on Titanium Substrate as a Silver Release System, Materials. 14 (2021) 4533. https://doi.org/10.3390/ma14164533.
[27] Z. Zhang, X. Cheng, Y. Yao, J. Luo, Q. Tang, H. Wu, S. Lin, C. Han, Q. Wei, L. Chen, Electrophoretic Deposition of Chitosan/Gelatin Coatings with Controlled Porous Surface Topography to Enhance Initial Osteoblast Adhesive Responses, J. Mater. Chem. B. 4 (2016) 7584–7595. https://doi.org/10.1039/C6TB02122K.
[28] Ł. Pawłowski, M. Bartmański, G. Strugała, A. Mielewczyk-Gryń, M. Jażdżewska, A. Zieliński. Electrophoretic Deposition and Characterization of Chitosan/Eudragit E 100 Coatings on Titanium Substrate, Coatings. 10 (2020) 607. https://doi.org/10.3390/coatings10070607.
[29] S. Ma, L. Guo, D. Dong, A Molecular Laser-Induced Breakdown Spectroscopy Technique for the Detection of Nitrogen in Water, J. Anal. At. Spectrom. 37 (2022) 663–667. https://doi.org/10.1039/D1JA00419K.
[30] A. Simchi, F. Pishbin, A.R. Boccaccini, Electrophoretic Deposition of Chitosan, Mater. Lett. 63 (2009) 2253–2256. https://doi.org/10.1016/j.matlet.2009.07.046.
[31] D.A. Al-ali, D. Al Groosh, M.H. Abdulkareem, The Influence of Chitosan on Adhesion of Silver Oxide Nanoparticles Coating on SS 316L in Biomedical Applications, JAMDSR. 10 (2022) 195–200.
[32] P.-Y. Lee, Y.-N. Chen, J.-J. Hu, C.-H. Chang, Comparison of Mechanical Stability of Elastic Titanium, Nickel-Titanium, and Stainless Steel Nails Used in the Fixation of Diaphyseal Long Bone Fractures, Mater. 11 (2018) 2159. https://doi.org/10.3390/ma11112159.
[33] K. Malisz, B. Świeczko-Żurek, A. Sionkowska, Preparation and Characterization of Diamond-like Carbon Coatings for Biomedical Application - A Review. Materials. 16 (2023) 3420. https://doi.org/10.3390/ma16093420.